Large-Angle X-ray Scattering Investigation of the Structure of 2-Propanol–Water Mixtures

Toshiyuki Takamuku, Kensuke Saisho, Sachiko Aoki, and Toshio Yamaguchi[a]

Department of Chemistry, Faculty of Science and Engineering, Saga University, Honjo-machi, Saga 840-8502, Japan

[a] Advanced Materials Institute and Department of Chemistry, Faculty of Science, Fukuoka University, Nanakuma, Jonan-ku, Fukuoka 814-0180, Japan

Reprint requests to Prof. T. T.; Fax: +81-952-28-8548; e-mail: takamut@cc.saga-u.ac.jp

Z. Naturforsch. **57 a,** 982–994 (2002); received March 18, 2002

The structure of 2-propanol and its aqueous mixtures has been investigated at 25 °C, using a large-angle X-ray scattering (LAXS) technique. The total radial distribution function of neat 2-propanol has shown that hydrogen-bonded chains of 2-propanol molecules are formed. In the 2-propanol-water mixtures, 2-propanol chains predominate at mole fractions $x_{2pr} > \sim 0.1$. When x_{2pr} decreases from $x_{2pr} = 1$, the number of hydrogen bonds reaches a plateau of 3.4 ± 0.1 at $x_{2pr} \leq \sim 0.1$, suggesting that the tetrahedral-like structure of water is mainly formed. On the basis of the present findings, together with previous results on methanol-water and ethanol-water mixtures, effects of hydrophobic groups on the structure of the alcohol-water mixtures are discussed. The heat of mixing at 25 °C as a function of x_{2pr} has been interpreted in terms of the structural transition of solvent clusters.

Key words: 2-Propanol–water Mixtures; Structure; LAXS; Hydrogen Bonds; Hydrophobic Group.

1. Introduction

Various physicochemical properties of aqueous aliphatic alcohols, such as heats of mixing [1], dielectric properties [2 - 5], and ^{1}H-NMR chemical shifts [6] have been measured. Anomalies in these properties have been found, e. g. the heats of mixing at 25 °C of aqueous methanol (M), ethanol (E), 1-propanol (1pr), and 2-propanol (2pr) show a minimum at the alcohol mole fractions $x_M = \sim 0.3$, $x_E = \sim 0.2$, $x_{1pr} = \sim 0.1$, and $x_{2pr} = \sim 0.1$, respectively [1, 7]. Such an alcohol dependence of physicochemical properties has often been interpreted in terms of the shape and size of hydrophobic groups.

The development of X-ray and neutron scattering techniques has enabled us to obtain direct information on the microscopic structure and interactions. Thus Nishikawa et al. [8 - 10] made small-angle X-ray scattering (SAXS) measurements on aqueous ethanol, 1-propanol, 2-propanol, and *tert*-butanol. D'Arrigo and Teixeira [11] performed small-angle neutron scattering (SANS) measurements on D_2O mixtures of 1-propanol, 2-propanol, *tert*-butanol, and butoxyethanol. Both the SAXS and SANS results showed that aggregates of either alcohol or alcohol-water complexes are formed, and that the size of aggregates significantly depends on the alcohol concentration and the shape and size of the hydrophobic groups. We have performed large-angle neutron scattering (LANS), LAXS, and mass spectrometric measurements on methanol [12], methanol-water [13], and ethanol-water [14 - 16] mixtures at various mole fractions. The results demonstrated that in methanol–water mixtures the tetrahedral-like structure of water moderately changes to hydrogen-bonded chains of methanol molecules at $x_M \approx 0.3$, while in ethanol-water mixtures a sharp change from the water network to ethanol chains takes place at $x_E \approx 0.2$. These findings suggest that the hydrophobic interactions among the ethyl groups disrupt the hydrogen-bonded network of water to stabilize the ethanol chains to the larger extent than the small methyl groups. Thus, the microscopic structure of aqueous 2-propanol mixtures is very important to understand the shape and size effects of hydrophobic groups. It has been reported from a Rayleigh light scattering experiment on 2-propanol–water mixtures [17], that a 2-propanol molecule is hydrated by 20 - 30 water molecules at

0932–0784 / 02 / 1200–0982 $ 06.00

$x_{2pr} = 0.05$, whereas 2-propanol clusters gradually appear in the mixtures with increasing x_{2pr}. However the microscopic structure of the 2-propanol–water mixtures has not yet been clarified over their whole mole fraction range.

In the present investigation we have made LAXS measurements on 2-propanol–water mixtures over the whole mole fraction range. On the basis of our results, a plausible structural change with the 2-propanol mole fraction is proposed. From a comparison with the structures of methanol–water and ethanol–water mixtures, effects of hydrophobic groups on mixing state of the alcohol–water mixtures are discussed. Finally, the heat of mixing at 25 °C as a function of x_{2pr} is interpreted from the structural changes proposed.

2. Experimental

2.1. Preparation of Samples

2-propanol (Wako Pure Chemicals, Grade for a high performance liquid chromatography) without further purification, and doubly distilled water were used for preparation of the samples. The densities of the solutions were measured with an electronic densimeter (ANTON Paar K. G. DMA 48).

2.2. LAXS Measurements

LAXS measurements for x_{2pr} = 0.03, 0.05, 0.07, 0.10, 0.20, 0.30, 0.40, 0.50, 0.60, 0.70, 0.80, 0.90, and 1 were carried out at 25 °C on a rapid X-ray diffractometer combined with an imaging plate (IP) as a two-dimensional detector (MAC Science, DIP301). Details and performance of the diffractometer have been described in [18, 19]. X-rays were generated at a rotary Mo anode operated at 50 kV and 200 mA, and then monochromatized by a flat graphite crystal to obtain Mo$K\alpha$ radiation (λ = 0.7107 Å). The sample solutions were sealed in glass capillaries of 2 mm inner diameter, and exposed to the X-rays for 1 h. The scattering angle (2θ) reached from 0.1° to 109°, corresponding to a scattering vector s (= $4\pi\lambda^{-1}\sin\theta$) of 0.02 to 14.4 Å^{-1}. The X-ray intensities for an empty capillary were also measured.

2.3. X-ray Data Treatment

Polarization and absorption corrections were first made for two-dimensional X-ray intensities, I_{obsd} (x,y), where x and y are vertical and horizontal coordinates of the IP, respectively, for a sample solution and an empty glass capillary as described in [18, 19]. Then, the two-dimensional intensities of $I_{obsd}(x, y)$ were integrated into one-dimensional data, $I_{obsd}(\theta)$, where 2θ is the scattering angle [18, 19]. The scattering intensities of the solutions alone were obtained by subtracting the intensities of the empty glass capillary from those of the samples. The corrected intensities were normalized to electron units in a stoichiometric volume containing one oxygen atom of 2-propanol and / or water by conventional methods [20 - 22]. A structure function, $i(s)$, and a radial distribution function (RDF) for each sample were obtained as described [15]. These treatments of the LAXS data were carried out with program KURVLR [23].

Quantitative analyses were performed on the LAXS data by the following two methods: 1.) A peak separation procedure in r-space with a Gaussian function, which was applied to a peak at ∼2.8 Å due mainly to the nearest-neighbor hydrogen bonded interaction. 2.) A comparison in s -space between experimental and theoretical structure functions based on a structural model.

In 1.) the RDF in the form of $D(r)/4\pi\rho_0$ was deconvoluted with Gaussian functions,

$$\frac{D_i^{calcd}(r)}{4\pi\rho_0} = \frac{A_i}{\sigma_i\sqrt{\pi/\ln 2}} \exp\left[-\ln 2\frac{r - r_{0i}}{\sigma_i}\right], \quad (1)$$

where A_i represents the peak area, r_{0i} the peak position, and σ_i the half-width at half-height of the peak for the i-th component of RDF. The peak area A_i corresponds to a coordination number, n, for an atom pair p-q. A comparison between the observed and calculated $D(r)$s was made by a least-squares fitting procedure to minimize the error square sum,

$$U = \frac{1}{4\pi\rho_0}\sum_{r_{min}}^{r_{max}}\left\{D^{obsd}(r) - \sum_i D_i^{calcd}(r)\right\}^2. \quad (2)$$

The parameters of A_i, r_{0i}, and σ_i were varied over the r-range from r_{min} to r_{max} during a least-squares refinement procedure.

A comparison in s-space between the experimental and model structure functions was performed over the s-range from s_{min} to s_{max} by a least-squares refinement procedure to obtain a minimum of the error square sum

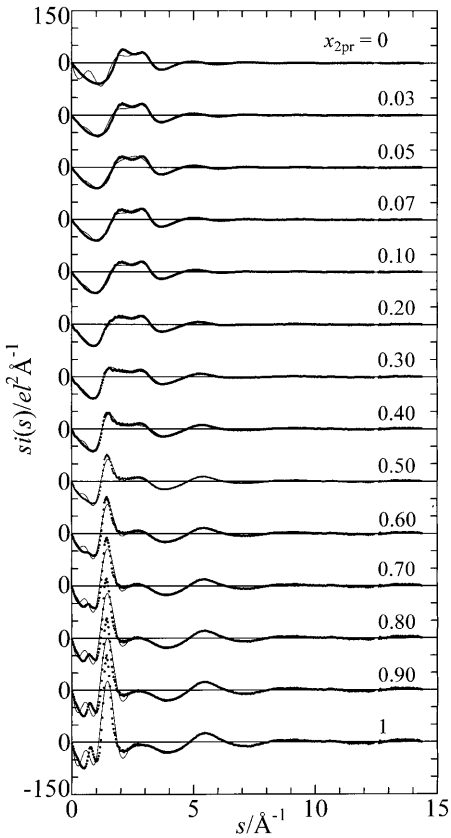

Fig. 1. Structure functions $i(s)$ multiplied by s for 2-propanol, water, and their mixtures at various 2-propanol mole fractions x_{2pr}. The dotted and solid lines are experimental and calculated ones, respectively.

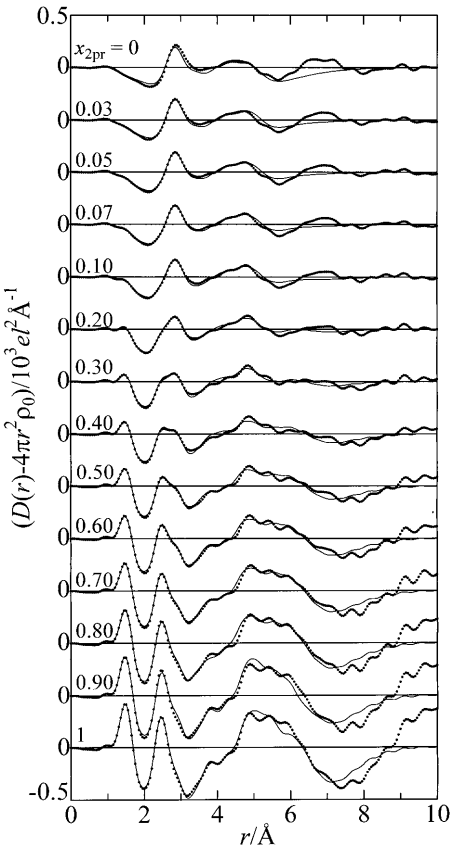

Fig. 2. Radial distribution functions in the form of $D(r) - 4\pi r^2\rho_0$ for 2-propanol, water, and their mixtures at various x_{2pr}. The dotted and solid lines are experimental and calculated ones, respectively.

$$U = \sum_{s_{min}}^{s_{max}} s^2 \left\{ i_{obsd}(s) - i_{calcd}(s) \right\}^2 . \quad (3)$$

The theoretical intensity, $i_{calcd}(s)$, was calculated by

$$i_{calcd}(s) = \sum_p \sum_q x_p n_{pq} f_p(s) f_q(s) \frac{\sin(r_{pq}s)}{r_{pq}s} \cdot \exp(-b_{pq}s^2) - \sum_p \sum_q x_p x_q f_p(s) f_q(s) \quad (4)$$

$$\cdot \frac{4\pi R_q^3}{V} \frac{\sin(R_q s) - R_q s \sin(R_q s)}{(R_q s)^3} \exp(-B_q s^2).$$

The first term of the right-hand side of (4) is related to the short-range interactions characterized by the interatomic distance r_{pq}, the temperature factor b_{pq}, and the number of interactions n_{pq} for an atom pair p-q. The second term arises from the interaction between a spherical hole and the continuum electron distribution beyond the hole. R_q is the radius of the spherical hole around atom q, and B_q is the softness parameter for emergence of the continuum electron distribution. In the least-squares refinement procedure on structure functions the computer program NLPLSQ [24] was used.

3. Results and Discussion

3.1. RDFs

Figure 1 shows s-weighted structure functions for neat 2-propanol and 2-propanol–water mixtures at various x_{2pr}, together with that for water [13] for comparison. The corresponding radial distribution functions (RDFs) in the form of $D(r) - 4\pi r^2\rho_0$ for the solutions are depicted in Figure 2.

Table 1. Intramolecular parameter values used for the analysis. The interatomic distance r (Å), the temperature factor b(Å^2), the number of interactions n.

Interaction	r	10^3b	n
2-propanol:			
O-H	0.965	5	1
C^1,C^3-C^2	1.526	1	2
C^1,C^3,C^2-H	1.114	1	7
C^2-O	1.430	1	1
C^1,C^3...O	2.395	1	2
C^1...C^3	2.532	1	1
O...H(C^2H)	2.056	5	1
O...H(C^1H_3)	2.679	5	2
	2.695	5	2
	3.382	5	2
Water [26]:			
O-H	0.970	2	2
H...H	1.555	10	1

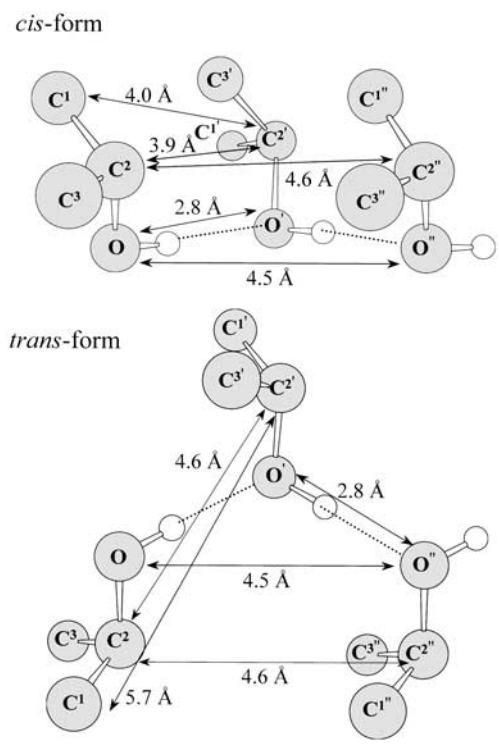

Fig. 3. Structure models of 2-propanol chains in *cis*- and *trans*-forms. The dotted lines represent hydrogen bonds.

Table 2. Important intermolecular parameter values for hydrogen bonded chains of 2-propanol molecules in *cis*- and *trans*-forms. The interatomic distance r (Å), the temperature factor b (Å^2), the number of interactions n per 2-propanol molecule.

Interaction	Parameter	— x_{2pr} = 1 — *cis*-form	*trans*-form
1st neighbor of 2-propanol–2-propanol:			
O...O	r	2.79	2.79
	10^3b	10	10
	n	1.7	1.7
C^2...O′	r	3.60	3.60
	10^3b	10	10
	n	1.7	1.7
C^2...$C^{2\prime}$	r	3.90	4.60
	10^3b	10	30
	n	0.85	0.85
C^2...$C^{1\prime}$	r	4.85	5.20
	10^3b	20	60
	n	0.85	0.85
C^2...$C^{3\prime}$	r	3.10	4.50
	10^3b	60	50
	n	0.85	0.85
C^1...O′	r	4.10	4.85
	10^3b	30	40
	n	1.7	0.85
C^1...$C^{2\prime}$	r	4.00	5.70
	10^3b	30	60
	n	0.85	0.85
C^3...O′	r	4.85	4.10
	10^3b	20	30
	n	0.85	0.85
2nd neighbor of 2-propanol–2-propanol:			
O...O″	r	4.50	4.50
	10^3b	40	40
	n	0.8	0.8
O...$C^{1\prime\prime}$	r	4.50	4.60
	10^3b	60	60
	n	0.8	0.8
O...$C^{3\prime\prime}$	r	4.60	4.50
	10^3b	60	60
	n	0.8	0.8
C^2...$C^{2\prime\prime}$	r	4.60	4.60
	10^3b	50	50
	n	0.8	0.8
C^1...O″	r	5.80	5.60
	10^3b	60	60
	n	0.8	0.8
$C^{1,3}$...$C^{1\prime\prime,3\prime\prime}$	r	4.60	4.60
	10^3b	60	60
	n	1.6	1.6

In the RDF for 2-propanol (x_{2pr} = 1), three peaks at 1.0, 1.4, and 2.4 Å originate from intramolecular interactions within a 2-propanol molecule. The first small peak at 1.0 Å arises from O-H and C-H bonds. The peaks at 1.4 and 2.4 Å are assigned to C^2-O and C^1-C^2 bonds and non-bonding C^1...C^3 and C^1...O interactions, respectively (see Fig. 3 for symbols of the atoms). To our knowledge, intramolecular structure parameters for a 2-propanol molecule determined by X-ray and neutron diffraction methods are not

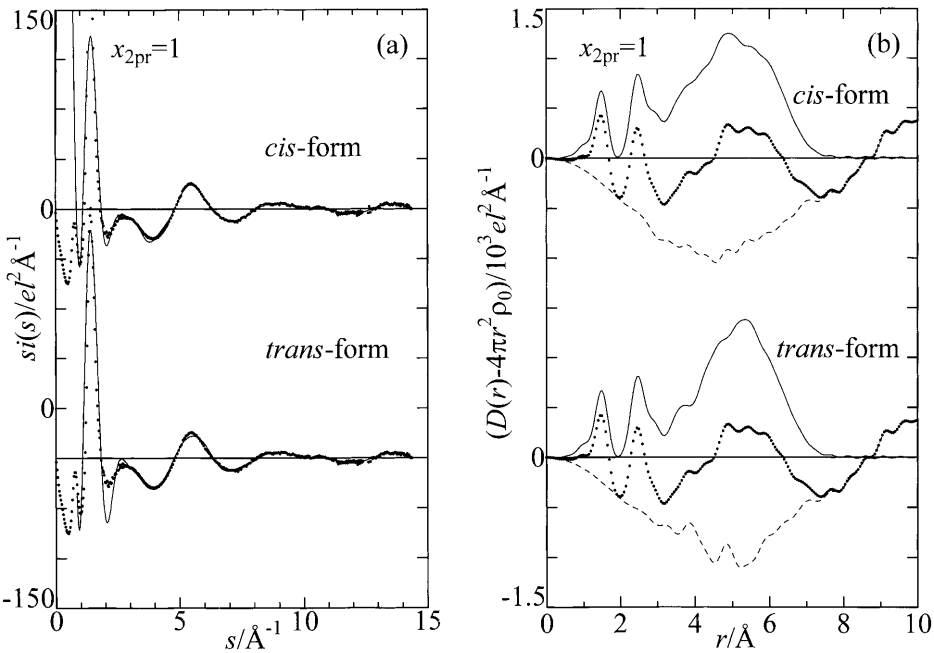

Fig. 4. The results of model fitting by *cis*- and *trans*-forms in (a) *s*- and (b) *r*-spaces. In the *s*-space the dotted and solid lines represent experimental and theoretical ones, respectively. In *r*-space the dotted and solid lines represent experimental and theoretical ones, and the dashed lines residual values obtained by subtraction of the theoretical ones from the experimental ones.

available in the literature and thus were estimated from those of an ethanol molecule previously determined from neutron diffraction measurements [25]. The structure parameters of a 2-propanol molecule employed in the present analysis are summarized in Table 1, together with those of water molecules [26]. The peaks beyond ∼2.8 Å arise mainly from intermolecular interactions among 2-propanol molecules. The shoulder at 2.8 Å is assigned to O...O hydrogen bonds between 2-propanol molecules. The large broad peak centered at ∼5 Å consists of various interactions for the first- and second-neighbors in a hydrogen-bonded chain of 2-propanol molecules. The broad peak beyond ∼8 Å is attributed to more distant-neighbor interactions, showing that hydrogen-bonded chains are formed to a large extent.

Since various conformations of a chain of 2-propanol molecules would be possible in the liquid, it is difficult to build up a unique model for the chain structure. Hence, two conformations of *cis*- and *trans*-forms were tested to see how they can explain the observed RDF at $r \leq$ ∼7 Å. In Fig. 3, models of the *cis*- and *trans*-forms are depicted with the important interatomic distances summarized in Table 2. In this figure, the interatomic distances of the first-neighbor molecule from a given central molecule are different from each other, i. e. ∼3.9 Å ($C^2...C^{2'}$) and ∼4.0 Å ($C^1...C^{2'}$) for the *cis*-form, and ∼4.6 Å and ∼5.7 Å, respectively, for the *trans*-form, but those of the second-neighbor molecule are similar in both forms, i. e. ∼4.5 Å (O...O") and ∼4.6 Å ($C^2...C^{2''}$) for both, the *cis*- and *trans*-forms. The results of the model fitting with the structure parameters in Table 2 are shown in Fig. 4 (a) and (b). As seen in Fig. 4 (a), both theoretical $si(s)$ values (solid lines) for the *cis*- and *trans*-forms satisfactorily explain the observed ones (dots) in the range of $s \geq$ ∼4 Å^{-1}, except for a small difference at ∼5 < s/Å^{-1} < ∼6 in the *trans*-form. In Fig. 4(b), the corresponding difference in the *s*-space is clearly observed in the RDFs. For the *cis*-form the residual curve (dashed line), which was obtained by subtracting the theoretical curve (solid line) from the observed one (dots), is smooth in the range of $r \leq$ ∼7 Å, suggesting that a model of the *cis*-form reproduce well the observed ones. On the other hand, for the *trans*-form two small peaks still remain at ∼3.9 and ∼4.9 Å in the residual curve. This is because the first-neighbor interactions between the *iso*-propyl groups,

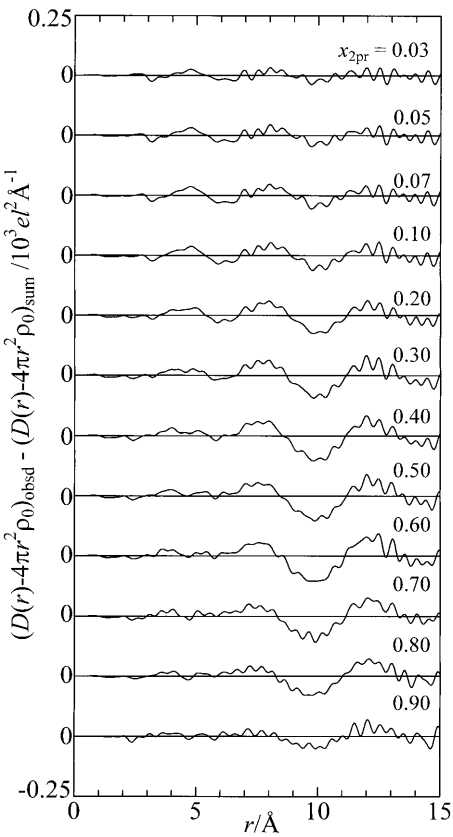

Fig. 5. Residual RDFs obtained from subtracting a weighted sum of RDFs for pure 2-propanol and pure water from the original RDFs.

such as $C^2 \ldots C^{2'}$ and $C^2 \ldots C^{1'}$, are too long in the *trans*-form. Although other conformations of hydrogen-bonded 2-propanol chains would be possible in the liquid, the present analysis shows that a hydrogen-bonded chain in the *cis*-form would be more favorable than that in the *trans*-form. This result implies that the hydrophobic interaction among the *iso*-propyl groups stabilizes the hydrogen-bonded chains in the mixtures because of the nearest hydrophobic interactions in the *cis*-form chains.

As seen in Fig. 2, for the 2-propanol–water mixtures the peak at 2.8 Å for O...O hydrogen bonds gradually increases with decreasing 2-propanol mole fraction (increasing water content). When the mole fraction x_{2pr} changes from 1 to 0.40, the broad peak centered at ∼5 Å for the first- and second-neighbor interactions in 2-propanol chains moderately decreases and shifts to ∼4.5 Å. In addition, the peak beyond ∼8 Å for the third- and fourth-neighbors in the 2-propanol chains is weakened with a decrease in x_{2pr} and almost disappears at x_{2pr} = 0.20. In the mole fraction range of $x_{2pr} \leq 0.10$, a new peak at ∼7 Å appears, which is due to the third-neighbor interactions in the tetrahedral-like structure of water [13, 27, 28]. The RDFs for the 2-propanol–water mixtures at $x_{2pr} \leq 0.10$ are well comparable with that for pure water (x_{2pr} = 0), where three peaks at 2.8, 4.5, and 7 Å, characteristic for the tetrahedral-like structure of water, are observed [13, 27, 28]. These features suggest that the inherent chain structure of 2-propanol molecules gradually decreases with decreasing mole fraction x_{2pr} from 1 to ∼0.10, and then the hydrogen-bonded network of water is mainly formed in the mixtures at $x_{2pr} \leq$ ∼0.10.

To emphasize the change in structure of the mixtures, the original RDFs for the 2-propanol–water mixtures were compared with a weighted sum of those for pure 2-propanol and pure water by

$$\left[D(r) - 4\pi r^2\rho_0\right]_{sum} = f_{2pr}\left[D(r) - 4\pi r^2\rho_{0,2pr}\right]_{2pr} + f_{Water}\left[D(r) - 4\pi r^2\rho_{0,Water}\right]_{Water}, \quad (5)$$

where $f_{2pr} = \rho_{0,Mix}/\rho_{0,2pr}$ and $f_{Water} = \rho_{0,Mix}/\rho_{0,Water}$ denote factors to correct differences in the average electron densities among the mixtures and pure liquids; $\rho_{0,Mix}$, $\rho_{0,2pr}$, and $\rho_{0,Water}$ represent the average electron densities in the stoichiometric volume for the mixtures, pure 2-propanol, and pure water, respectively. The sum RDF thus obtained was subtracted from the original RDF, and the residual RDFs are shown in Figure 5. Over the whole mole fraction range only a very weak peak and a shallow valley are observed in the *r*-range from 0 to 7 Å. However, at $x_{2pr} \leq$ ∼0.20 a small peak is discernible at 3.5 - 5.5 Å, suggesting that new interactions, such as hydrogen bonds between 2-propanol and water molecules, are formed in the mixtures. Above 7 Å, a broad peak at ∼8 Å appears at x_{2pr} = 0.60 and gradually grows with decreasing 2-propanol mole fraction to ∼0.20. This enhancement of the 8 Å peak might be attributed to a small change in the conformation of the hydrogen-bonded 2-propanol chains for pure 2-propanol. In addition, a valley centered at ∼10 Å, where the third- and fourth-neighbor interactions among 2-propanol molecules contribute, is observed in the residual RDFs, suggesting a decrease in 2-propanol oligomers with increasing water content.

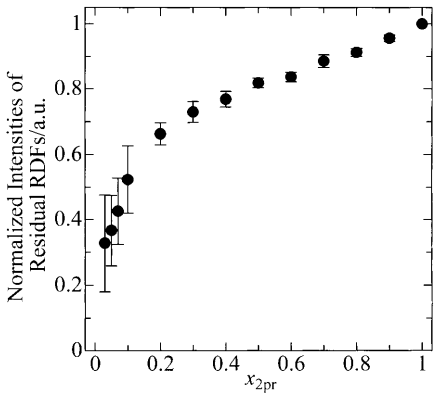

Fig. 6. Intensities of the residual RDFs at $9.5 \leq r/\text{Å} \leq 10.5$, which are normalized by the 2-propanol content. The standard deviations of σ values are given as error bars.

Here, the valley at ∼10 Å was quantitatively examined as follows. The negative intensities of the valley at 9.5 - 10.5 Å in the RDFs were averaged for each mixture and then normalized by x_{2pr} to cancel the concentration dependence. The normalized intensities can be regarded as ratios of 2-propanol oligomers formed in the mixtures to those in pure 2-propanol. In Fig. 6 the estimated ratios are plotted as a function of x_{2pr}. As shown in this figure, the ratios gradually decrease with decreasing x_{2pr} to ∼0.2, revealing a decrease in 2-propanol oligomers. At $x_{2pr} \leq 0.1$ the ratios contain large uncertainties because of low 2-propanol concentration, but it appears that the ratio drastically decreases with decrease in x_{2pr} from 0.1 to 0.03. These results are consistent with that obtained from the original RDFs, i.e. the hydrogen-bonded 2-propanol chains are predominantly formed in the 2-propanol–water mixtures at $x_{2pr} > \sim 0.1$, while the tetrahedral-like structure of water evolves in the mixtures at $x_{2pr} \leq \sim 0.1$.

3.2. Peak Separation Procedure

To quantify the O...O hydrogen bonds formed in the 2-propanol–water mixtures, a peak separation procedure was performed for the RDFs in the form of $D(r)/4\pi\rho_0$ over the r-range from 2.30 to 4.25 Å, through (1) and (2). Figure 7 shows typical results of the peak fitting procedure on the RDFs. As seen in Fig. 7, three Gaussian components contribute to the observed RDFs over the whole mole fraction range; the first component (I) at ∼2.8 Å is due to hydrogen bonds of 2-propanol–2-propanol, 2-propanol–water,

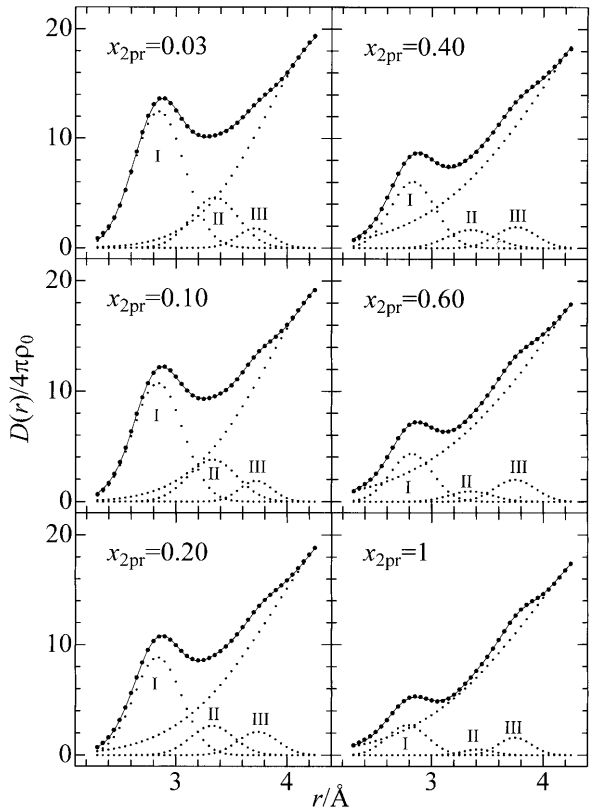

Fig. 7. Examples of the peak separation analysis on radial distribution functions (RDFs). The experimental values are given by filled circles, each component deconveluted by dots, and the total theoretical values by solid lines.

and water–water molecules, the second component (II) at ∼3.4 Å is due to $C^1 \ldots C^{3'}$ and $C^2 \ldots C^{3'}$ interactions in the *cis*-formed 2-propanol chains and non-hydrogen bonded O...O interaction related to the interstitial water molecules [13, 18, 27, 28], and the third one (III) centered at ∼3.7 Å of $C^2 \ldots O'$ and $C^2 \ldots C^{2'}$ interactions of the first-neighbors in the *cis*-formed 2-propanol–chains and C...O interaction between 2-propanol and water molecules within the hydrophobic hydration shell around the *iso*-propyl group [29]. In the present analysis the longer-range interactions beyond ∼3.7 Å were treated as a background. The parameters of r_{0i}, σ_i, and A_i in (1) for the i-th Gaussian component were refined through the least-squares fitting procedure with (2). Here, the peak area A_i corresponds the coordination number of an atom pair p-q. In the calculations, the parameters of r_{0i}, σ_i, and A_i for each component were influenced by those for background and a maximum distance r_{max}

Table 3. Optimized parameter values from a peak separation procedure applied to RDFs for water, 2-propanol, and their mixtures at various 2-propanol mole fractions. The intermolecular distance r (Å), the half-width at half-height of the peak σ (Å), and the coordination number n. The values in parentheses are estimated standard deviations of the last figure.

	Hydrogen bond O...O		
x_{2pr}	r	σ	n
0 [13]	2.87 (1)	0.29 (1)	3.4 (1)
0.03	2.85 (1)	0.27 (1)	3.4 (1)
0.05	2.84 (1)	0.26 (1)	3.4 (1)
0.07	2.84 (1)	0.26 (1)	3.4 (1)
0.10	2.84 (1)	0.26 (1)	3.4 (1)
0.20	2.84 (1)	0.25 (1)	3.3 (1)
0.30	2.84 (1)	0.24 (1)	3.1 (1)
0.40	2.83 (1)	0.24 (1)	2.9 (1)
0.50	2.83 (1)	0.23 (1)	2.6 (1)
0.60	2.82 (1)	0.22 (1)	2.4 (1)
0.70	2.81 (1)	0.22 (1)	2.2 (1)
0.80	2.81 (1)	0.21 (1)	2.1 (1)
0.90	2.80 (1)	0.21 (1)	2.0 (1)
1	2.79 (1)	0.21 (1)	2.0 (1)

in the fits. Thus, preliminary fits were made by varying r_{max} from 4.00 to 4.50 Å. The results of the fits revealed that when the r_{max} was beyond 4.25 Å, the observed RDFs could not be reproduced by only four components. Thus the r_{max} value of 4.25 Å was employed, and the parameter values for the background were fixed to reproduce the observed curve within 4.00 to 4.25 Å in each RDF. Finally, the parameters for each component were optimized by using (2). The optimized parameters r, σ, and n of hydrogen bonds (component I) are given in Table 3 with the estimated uncertainties ±0.01 Å, ±0.01 Å, and ±0.1, respectively. As seen in Fig. 7, the theoretical RDFs calculated from the final values reproduce well the observed ones.

Table 3 shows that the length (2.79 ± 0.01) Å of O...O hydrogen bonds for pure 2-propanol is comparable with that (2.76 ± 0.01) Å for methanol previously determined [13]. When x_{2pr} decreases from 1 to 0, the length of the hydrogen bond gradually increases from (2.78 ± 0.01) to (2.87 ± 0.01) Å. A similar change in the length of hydrogen bonds was observed for methanol–water mixtures [13].

For pure 2-propanol, the number (2.0 ± 0.1) of hydrogen bonds is compared with those (1.9 ± 0.1) for methanol [13] and ethanol [16], suggesting that 2-propanol molecules form linear hydrogen-bonded chains in pure 2-propanol with a similar size of the

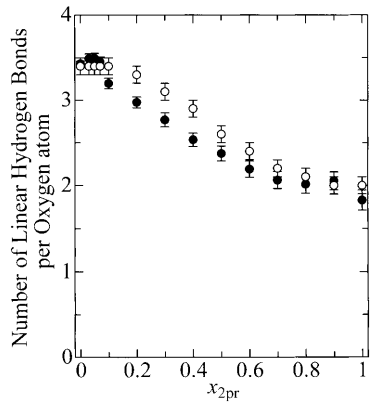

Fig. 8. The coordination number per oxygen atom within both 2-propanol and water molecules as a function of the 2-propanol mole fraction. The values determined by a peak separation procedure are given by opened circles, those from a least-squares refinement by filled circles, together with the standard deviation of σ values as error bars.

chain in methanol and ethanol. The number of hydrogen bonds n is depicted as a function of x_{2pr} in Figure 8. As shown in Fig. 8, the number of hydrogen bonds increases when x_{2pr} decreases, but does not monotonously change with the mole fraction. In the x_{2pr}-range from 1 to ∼0.70 the number of hydrogen bonds slowly increases with decreasing x_{2pr}, but quickly at x_{2pr} below 0.70. Finally, at $x_{2pr} \leq \sim 0.1$ the value reaches a plateau of $\sim 3.4 \pm 0.1$, which agrees with the value ($\sim 3.4 \pm 0.1$) determined for pure water [13]. This change in the number of hydrogen bonds with the mole fraction leads to two inflection points at $x_{2pr} \approx 0.10$ and 0.70. The inflection point at $x_{2pr} \approx 0.10$ in the number of hydrogen bonds is comparable with that in the decrease in 2-propanol oligomers with mole fraction (Fig. 6). This coincidence strongly suggests a change in structure of the 2-propanol-water mixtures at $x_{2pr} \approx 0.10$. On the other hand, the inflection point at $x_{2pr} \approx 0.70$ may arise mainly from a change in the number of hydrogen bonds among water molecules because the corresponding inflection point is scarcely discernible in Figure 6.

3.3. Least-squares Refinements for Structure Functions

A model fitting procedure through (3) and (4) was performed on the structure functions for neat 2-propanol and 2-propanol–water mixtures (Fig. 1) to evaluate the long-range interactions of 2-propanol–2-propanol, 2-propanol–water, and water–water in the so-

Table 4. Important optimized parameter values of the interactions in water, 2-propanol and their mixtures by a least-squares refinement on structure functions over the s-range $0.1 \leq s/\text{Å}^{-1} \leq 14.4$. The interatomic distance r (Å), the temperature factor b (Å^2), the number of interactions n per 2-propanol molecule. The values in parentheses are standard deviations of the last figure. The parameters without standard deviations were not allowed to vary in the calculations.

								— x_{2pr} —							
Inter-action	Para-meter	0 [13]	0.03	0.05	0.07	0.10	0.20	0.30	0.40	0.50	0.60	0.70	0.80	0.90	1
Linear hydrogen bond of water–water, 2-propanol–water, and 2-propanol–2-propanol															
O...O	r	2.826 (2)	2.817 (3)	2.815 (3)	2.816 (3)	2.811 (3)	2.805 (4)	2.800 (5)	2.794 (5)	2.788 (6)	2.778 (7)	2.762 (8)	2.747 (9)	2.734 (9)	2.736 (11)
	10^3b	17	17	17	17	17	17	17	15	12	12	12	10	10	10
	n	3.43(3)	3.49(6)	3.49(6)	3.45(6)	3.20(6)	2.97(6)	2.77(8)	2.53(8)	2.37(9)	2.19(9)	2.06(10)	2.01(10)	2.05(10)	1.83(12)
Interstitial water molecules															
O···O	r	3.35	3.35	3.35	3.35	3.35	3.35	3.35	3.35	3.35	3.35	3.35			
	10^3b	15	20	20	20	30	30	30	30	30	30	30			
	n	1.0	1.25	1.24	1.22	1.08	0.83	0.70	0.77	0.68	0.49	0.30			
2nd neighbor of water–water															
O···O	r	4.00	4.00	4.00	4.00	4.00	4.00	4.00	4.00						
	10^3b	90	40	40	40	40	40	40	40						
	n	3.0	2.4	2.4	2.4	2.4	2.4	2.4	2.4						
2nd neighbor of water–water and 2-propanol–water															
O···O	r	4.50	4.50	4.50	4.50	4.50	4.50	4.50	4.50	4.50	4.50	4.50	4.50	4.50	
	10^3b	90	40	40	40	40	40	40	40	40	40	40	40	40	
	n	3.0	2.0	2.0	2.0	2.0	2.0	1.8	1.6	1.4	1.3	1.1	0.8	0.6	
1st neighbor of 2-propanol–2-propanol															
$C^2\cdots C^{2\prime}$	r		3.90	3.90	3.90	3.90	3.90	3.90	3.90	3.90	3.90	3.90	3.90	3.90	3.90
	10^3b		10	10	10	10	10	10	10	10	10	10	10	10	10
	n		0.85	0.85	0.85	0.85	0.85	0.85	0.85	0.85	0.85	0.85	0.85	0.85	0.85
$C^1\cdots O'$	r		4.10	4.10	4.10	4.10	4.10	4.10	4.10	4.10	4.10	4.10	4.10	4.10	4.10
	10^3b		30	30	30	30	30	30	30	30	30	30	30	30	30
	n		1.7	1.7	1.7	1.7	1.7	1.7	1.7	1.7	1.7	1.7	1.7	1.7	1.7
$C^3\cdots O'$	r		4.85	4.85	4.85	4.85	4.85	4.85	4.85	4.85	4.85	4.85	4.85	4.85	4.85
	10^3b		20	20	20	20	20	20	20	20	20	20	20	20	20
	n		0.85	0.85	0.85	0.85	0.85	0.85	0.85	0.85	0.85	0.85	0.85	0.85	0.85
2nd neighbor of 2-propanol–2-propanol															
$O\cdots O''$	r		4.50	4.50	4.50	4.50	4.50	4.50	4.50	4.50	4.50	4.50	4.50	4.50	4.50
	10^3b		40	40	40	40	40	40	40	40	40	40	40	40	40
	n		0.8	0.8	0.8	0.8	0.8	0.8	0.8	0.8	0.8	0.8	0.8	0.8	0.8
$C^2\cdots C^{2\prime\prime}$	r		4.60	4.60	4.60	4.60	4.60	4.60	4.60	4.60	4.60	4.60	4.60	4.60	4.60
	10^3b		50	50	50	50	50	50	50	50	50	50	50	50	50
	n		0.8	0.8	0.8	0.8	0.8	0.8	0.8	0.8	0.8	0.8	0.8	0.8	0.8

lutions and confirm the number of hydrogen bonds estimated from the peak separation procedure in the r-space as described in the previous section. In the present analysis the structure parameters of the intramolecular interactions 2-propanol and water [26] molecules as listed in Table 1 were fixed during the analysis.

For pure 2-propanol, as discussed in the previous section, the total RDF in the r-range from ∼2 to ∼7 Å can be explained by the structure model of the *cis*-formed 2-propanol chain. Thus, the structure parameters for the *cis*-formed chain listed in Table 2 were used as plausible model parameters in the least-squares refinement procedure. However, the long-range interactions beyond ∼7 Å were not taken into account because of their complexity; instead, continuum electron distributions for the individual atoms were introduced. For the 2-propanol–water mixtures, as described in the previous section, the residual RDFs suggest that the sum of RDFs of pure 2-propanol and pure water does not completely explain the total RDFs for the mixtures. Thus, to search for the most

likely structure model, the structure parameters of the *cis*-formed 2-propanol chain and the tetrahedral-like structure of water, together with non-hydrogen bonding interstitial molecules [13], were modified to fit well the total RDFs for $r \leq \sim 7$ Å. The most likely structure models could be obtained only by modifying the numbers of interactions and the temperature factors concerned with O...O hydrogen bonds between 2-propanol and water molecules, the tetrahedral-like structure of water, and the interstitial water molecules, but the parameters for the 2-propanol chains were fixed to the values in Table 2 during the calculation. Continuum electron distributions were introduced to the longer-range interactions beyond ~7 Å because the corresponding interactions are too complex to be uniquely determined. Finally, the least-squares fitting procedure was applied to the structure functions over the *s*-range from 0.1 to 14.4 $Å^{-1}$ by using the model parameters preliminary obtained.

In Table 4 the important optimized values are summarized. As seen in Figs. 1 and 2, the theoretical $si(s)$ and RDFs calculated by using the optimized values reproduce well the observed ones, except for the *s*-range of $s < \sim 3$ $Å^{-1}$ and the *r*-range of $r > \sim 7$ Å, where the corresponding long-range interactions were not taken into account in the present analysis. The distance (2.736 ± 0.011) Å and the number (1.83 ± 0.12) of O...O hydrogen bonds for pure 2-propanol are comparable with those (2.79 ± 0.01 Å and 2.0 ± 0.1) obtained from the peak separation procedure in the *r*-space. Furthermore, the distance and number of O...O hydrogen bonds are compared with those (2.771 ± 0.004 Å and 1.73 ± 0.03) determined for methanol in the previous investigation [13]. For the 2-propanol-water mixtures, the distances estimated in the *s*-space fits are slightly different from those by the peak separation procedure in the *r*-space, e. g. at x_{2pr} = 0.50 the distance was estimated to be (2.788 ± 0.006) Å from the former, but (2.83 ± 0.01) Å from the latter. These differences in the O...O distances may be attributed to uncertainties inherent in both methods. However, the change in the O...O distance and x_{2pr} agree well with each other; the distance of O...O hydrogen bonds gradually increases with increasing water content. The same tendency for the O...O distance was observed for methanol–water mixtures as reported in [13]. The difference of the O...O distance between alcohol and water may arise from the different number of hydrogen bonds per oxygen atom between water and alcohol molecules; the O...O distance for water molecules, hydrogen-bonded with four molecules, is slightly longer than that for alcohol molecules bonded with two or three molecules. Thus, the more the tetrahedral-like structure of water is formed in the mixtures, the longer the O...O distance is estimated for the alcohol–water mixtures.

As seen in Table 4, with x_{2pr} from 1 to 0, the number of O...O hydrogen bonds for the 2-propanol–water mixtures gradually increases from 1.83 ± 0.12 to 3.43 ± 0.03. In Fig. 8 the numbers of hydrogen bonds for the 2-propanol-water mixtures estimated from the least-squares fits in *s*-space are plotted as a function of x_{2pr}, together with those from the peak separation procedure in *r*-space for comparison. Figure 8 shows that the numbers of O...O hydrogen bonds obtained from both methods satisfactorily agree, but the systematic differences beyond the uncertainties estimated are shown. It is probable that the differences arise from ambiguities not completely eliminated from both analyses, such as corrections among structural model parameters employed. However, a similar change in the number of O...O hydrogen bonds with x_{2pr} is observed in each plot; 1.) the number of O...O hydrogen bonds moderately increases with decreasing of x_{2pr} down to ~0.7, 2.) in the mole fraction range of $0.1 \leq x_{2pr} < \sim 0.7$ it proportionally increases with decreasing x_{2pr}, and 3.) almost saturates to ~3.4 at $x_{2pr} < \sim 0.1$, leading to two inflection points at $x_{2pr} \approx 0.1$ and 0.7. In particular, the inflection point at $x_{2pr} \approx 0.1$ agrees well with that for the decrease in 2-propanol oligomers with decreasing x_{2pr} (Fig. 6). These inflection points suggest that a structural change in the 2-propanol–water mixtures occurs in three regimes; $0 < x_{2pr} \leq \sim 0.7$, $\sim 0.1 < x_{2pr} < \sim 0.7$, and $x_{2pr} \leq \sim 0.1$. For methanol–water [13] and ethanol–water [16] mixtures in the previous investigation, the inflection points for the number of O...O hydrogen bonds were observed at methanol mole fractions, $x_M \approx 0.3$ and 0.7 and ethanol mole fractions, $x_E \approx 0.2$, respectively. The present and previous results clearly reveal that the structural transition of solvent clusters in alcohol–water mixtures depends on the size of the alkyl groups.

3.4. Structure of 2-Propanol–Water Mixtures

In pure 2-propanol oligomers of 2-propanol molecules form hydrogen-bonded chains, where hydrophobic interactions among *iso*-propyl groups will

play an important role for stabilization of the chain. When water is added to 2-propanol, the inherent structure observed for pure 2-propanol does not drastically change in the 2-propanol-water mixtures at $\sim 0.7 \leq x_{2pr} < 1$. With further decreasing x_{2pr} from $\sim$0.7 to $\sim$0.1, the 2-propanol oligomers are moderately disrupted in the mixtures, whereas the hydrogen bonds among water molecules gradually increase. It is probable that hydrogen bonds between water molecules and terminal 2-propanol molecules in the chains are also formed in the mixtures. Nevertheless, the inherent structure of 2-propanol at the first- and second-neighbors is kept for $x_{2pr} > \sim 0.1$. It is thus suggested that both 2-propanol and water aggregates coexist in the mixtures at $\sim 0.1 < x_{2pr} < \sim 0.7$. At $x_{2pr} \leq \sim 0.1$, finally, the tetrahedral-like structure of water is predominantly formed. The 2-propanol molecules could be hydrated into the hydrogen-bonded network of water in the mixtures at $x_{2pr} \leq \sim 0.1$. This result agrees well with the previous conclusion from Rayleigh light scattering investigation; a 2-propanol molecule is hydrated by 20 - 30 water molecules in 2-propanol–water mixture at $x_{2pr} = 0.05$ [17]. In addition, the present conclusion is consistent with the results of 2-propanol–water mixtures at undercooled temperatures by a differential scanning calorimetry; water ice crystallizes in the mixtures at $x_{2pr} \leq 0.13$, while hydrated 2-propanol aggregates are formed at $x_{2pr} > 0.13$ [30].

Both the present and previous results have shown the size effect on the mixing state of alcohol and water molecules. The larger the hydrophobic groups, the more rapidly the hydrogen-bonded network of water is disturbed with increasing alcohol content, i. e. the change from the water structure to alcohol molecule chains takes place at alcohol mole fractions of $\sim$0.1, $\sim$0.2, and $\sim$0.3 in aqueous mixtures of 2-propanol, ethanol, and methanol, respectively. Moreover, in methanol–water mixtures the structural transition of solvent clusters occurs moderately as water molecules in the hydrogen-bonded network are gradually replaced by methanol molecules with increasing methanol content, whereas in aqueous mixtures of 2-propanol and ethanol the change from the water network to hydrogen-bonded alcohol chains sharply occurs. This is because the hydrophobic interaction among the alkyl groups, such as the *iso*-propyl and ethyl groups, makes aggegation of 2-propanol and ethanol molecules easy in aqueous mixtures. In fact, a low-frequency Raman spectroscopic investigation on aqueous mixtures of several aliphatic alcohols showed that microheterogeneity occurs in 2-propanol–water and ethanol-water mixtures, but does not in methanol-water mixtures [31].

3.5. Heat of Mixing

The heat of mixing for 2-propanol–water mixtures at 25 °C is negative at $x_{2pr} < \sim 0.5$, but positive at $x_{2pr} > \sim 0.5$, with a minimum (–650 J mol^{-1}) at $x_{2pr} \approx 0.1$ and a maximum (225 J mol^{-1}) at $x_{2pr} \approx 0.7$ [7]. The inflection points at $x_{2pr} \approx 0.1$ and 0.7 correspond well to the structural transition of 2-propanol-water mixtures as shown in Figure 8.

In the range of $x_{2pr} \leq \sim 0.1$, the tetrahedral-like structure of water predominates in 2-propanol–water mixtures. Molecular dynamics simulations on several *n*-alcohol-water mixtures [32, 33] and a neutron diffraction investigation on *tert*-butanol-water mixtures [34] revealed that the number of hydrogen bonds between alcohol and water molecules via the hydroxyl group increases at low alcohol content, resulting in stabilization of alcohol molecule. When 2-propanol molecules are added to water, they will also be stabilized in the tetrahedral-like structure of water through hydrogen bonds between 2-propanol and water molecules, and an enthalpic gain due to the stabilization of 2-propanol molecules is largest at $x_{2pr} \approx 0.1$. For methanol–water and ethanol–water mixtures, the minima of the heats of mixing are observed at $x_M \approx 0.3$ and $x_E \approx 0.2$, respectively, where the structural transition of dominant clusters from the tetrahedral-like structure of water to hydrogen-bonded alcohol chains takes place [13, 15]. Thus, the minimum of the heat of mixing of 2-propanol–water mixtures is observed at the lowest alcohol content among the mixtures. This because the largest hydrophobic group of the 2-propanol molecule most quickly disrupts the tetrahedral-like structure of water with increasing alcohol content. In addition, the minimum of the heat of mixing for the alcohol–water mixtures is less negative in the sequence of 2-propanol (–650 J mol^{-1}) > ethanol (–730 J mol^{-1}) > methanol (–850 J mol^{-1}) [1, 7] because the enthalpic gain of the stabilization of 2-propanol is most significantly canceled by the disruption of the water structure among the alcohols.

On the other hand, in the range of $x_{2pr} > \sim 0.1$, the tetrahedral-like structure of water is gradually disrupted by dominant 2-propanol chains with increasing 2-propanol content. Hence the heat of mixing

becomes less negative with increasing x_{2pr}. When x_{2pr} exceeds ∼0.5, the heat of mixing for 2-propanol–water mixtures becomes positive, while those for methanol–water and ethanol–water mixtures are still negative over the whole alcohol mole fraction range. This may arise from a difference in the strength of hydrogen bond between alcohol molecules. It was concluded from the low-frequency Raman spectroscopic investigation [31] that the hydrogen bonds between alcohol molecules is weakened in the sequence methanol > ethanol > 2-propanol. For 2-propanol-water mixtures an enthalpic gain of formation of hydrogen bonds between 2-propanol molecules will be not enough to cancel the enthalpic loss of disruption of the hydrogen bonds among water molecules. On the other hand, the hydrogen bonding of methanol and ethanol molecules is still sufficient to compensate the enthalpic loss of disruption of the hydrogen bonds among the water molecules. In the range of $x_{2pr} \geq \sim 0.7$, 2-propanol chains predominate in 2-propanol–water mixtures, while the tetrahedral-like structure of water is scarcely formed. The formation of the hydrogen-bonded 2-propanol chains significantly contributes to the heat of mixing because most hydrogen bonds among water molecules are disrupted. Thus, the heat of mixing for 2-propanol–water mixture decreases again with increasing x_{2pr}, resulting in the maximum of the heat of mixing at $x_{2pr} \approx 0.7$.

4. Conclusion

The present results of LAXS measurements have shown the change in the structure of 2-propanol–water mixtures with x_{2pr}; the tetrahedral-like structure of water is predominantly formed at $x_{2pr} \leq \sim 0.1$, both water network and 2-propanol chains coexist in mixtures of $\sim 0.1 < x_{2pr} < \sim 0.7$, and the 2-propanol chains are the dominant species in the mixtures at $x_{2pr} > \sim 0.7$. It has been concluded that the structural transitions of dominant clusters in 2-propanol-water mixtures correspond well to the anomalies of the heat of mixing at 25 °C as a function of x_{2pr}. A comparison among the structures of 2-propanol–water, methanol–water, and ethanol–water mixtures has revealed that the effects of the hydrophobic group on the mixing state of the alcohol and water molecules are cooperative in disrupting the hydrogen-bonded structure of water and aggregating of alcohol molecules.

Acknowledgement

The present work was supported in part by Grants-in-Aid (No.09740444 and No.12640500) from the Ministry of Education, Culture, Sports, Science, and Technology, Japan.

[1] F. Franks and D. J. G. Ives, Q. Rev. Chem. Soc. **20**, 1 (1966).
[2] S. Mashimo, S. Kuwabara, S. Yagihara, and K. Higasi, J. Chem. Phys. **90**, 3292 (1989).
[3] N. Asaka, N. Shinyashiki, T. Umehara, and S. Mashimo, J. Chem. Phys. **93**, 8273 (1990).
[4] S. Mashimo, T. Umehara, and H. Redlin, J. Chem. Phys. **95**, 6257 (1991).
[5] T. Takei, C. Amano, Y. Nishimoto, and Y. Sugitani, Anal. Sci. **13**, 1043 (1997).
[6] A. Coccia, P. L. Inodovia, F. Podo, and V. Viti, Chem. Phys. **7**, 30 (1975).
[7] F. Franks, Water: A Comprehensive Treaties Vol. 2, Plenum Press, New York 1973, p. 357.
[8] K. Nishikawa, H. Hayashi, and T. Iijima, J. Phys. Chem. **93**, 6559 (1989).
[9] H. Hayashi, K. Nishikawa, and T. Iijima, J. Phys. Chem. **94**, 8334 (1990).
[10] K. Nishikawa and T. Iijima, J. Phys. Chem. **97**, 10824 (1993).
[11] G. D'Arrigo and J. Teixeira, J. Chem. Soc. Faraday Trans. **86**, 1503 (1990).
[12] T. Yamaguchi, K. Hidaka, and A. K. Soper, Mol. Phys. **96**, 1159 (1999); T. Yamaguchi, K. Hidaka, and A. K. Soper, Mol. Phys. **97**, 603 (1999).
[13] T. Takamuku, T. Yamaguchi, M. Asato, M. Matsumoto, and N. Nishi, Z. Naturforsch. **55a**, 513 (2000).
[14] N. Nishi, S. Takahashi, M. Matsumoto, A. Tanaka, K. Muraya, T. Takamuku, and T. Yamaguchi, J. Phys. Chem. **99**, 462 (1995).
[15] M. Matsumoto, N. Nishi, T. Furusawa, M. Saita, T. Takamuku, M. Yamagami, and T. Yamaguchi, Bull. Chem. Soc. Japan **68**, 1775 (1995).
[16] N. Nishi, M. Matsumoto, S. Takahashi, T. Takamuku, M. Yamagami, and T. Yamaguchi, Structures and Dynamics of Clusters, T. Kondow, K. Kaya, and A. Terasaki, ed., Universal Academy Press, Inc. and Yamada Science Foundation, 1996, pp.113-120.

[17] Y. G. Wu, M. Tabata, and T. Takamuku, Talanta **54**, 69 (2001).
[18] K. Yamanaka, T. Yamaguchi, and H. Wakita, J. Chem. Phys. **101**, 9830 (1994).
[19] M. Ihara, T. Yamaguchi, H. Wakita, and T. Matsumoto, Adv. X-Ray Anal. Japan **25**, 49 (1994); T. Yamaguchi, H. Wakita, and K. Yamanaka, Fukuoka Univ. Sci. Reports **29**, 127 (1999).
[20] K. Furukawa, Rep. Progr. Phys. **25**, 395 (1962).
[21] J. Krogh-Moe, Acta Crystallogr. **2**, 951 (1956).
[22] N. Norman, Acta Crystallogr.**10**, 370 (1957).
[23] G. Johanson and M. Sandström, Chem. Scr. **4**, 195 (1973).
[24] T. Yamaguchi, Doctoral Thesis, Tokyo Institute of Technology, 1978.
[25] Y. Tanaka, N. Ohtomo, and K. Arakawa, Bull. Chem. Soc. Japan **57**, 2569 (1984).
[26] K. Ichikawa, Y. Kameda, T. Yamaguchi, H. Wakita, and M. Misawa, Mol. Phys. **73**, 79 (1991).
[27] A. H. Narten and H. A. Levy, J. Chem. Phys. **55**, 2263 (1971).
[28] A. H. Narten, J. Chem. Phys. **56**, 5681 (1972).
[29] A. K. Soper and J. L. Finney, Phys. Rev. Lett. **71**, 4346 (1993).
[30] K. Takaizumi, J. Solution Chem. **29**, 377 (2000).
[31] K. Yoshida and T. Yamaguchi, Z. Naturforsch. **56a**, 529 (2001).
[32] G. Pálinkás and I. Bakó, Z. Naturforsch. **46a**, 95 (1991).
[33] J. Fidler and P. M. Rodger, J. Phys. Chem. B **103**, 7695 (1999).
[34] D. T. Bowron, J. L. Finney, and A. K. Soper, J. Phys. Chem. B **102**, 3551 (1998).